



Diagnosis of Inflammations of the Paranasal Sinuses and Nasal Cavities in Deep Learning CNN Model

Ms. Minal Pawar¹, Ms. Rani Patil², Mr. Deepak Pandita³, D.Snehal Bhagajirao Godse⁴, Mr.Mahesh Kadam⁵, Mrs. Pallavi S.Thorat⁶

^{1,2}Dr. D.Y. Patil School of Science and Technology, Tathwade, Pune, Maharashtra, India

^{3,6}Pimpri Chinchwad University School of Engineering and Technology, Pune, Maharashtra, India

^{4,5}JSPM's Rajarshi Shahu College of Engineering, Department of MCA, Tathawade, Pune, India

Emails: rani.patil@dpu.edu.in², pandita.deep@gmail.com³

Abstract

Diagnostic histopathology is crucial for identifying fungal sinusitis, which can include allergic fungal sinusitis and nasal eosinophilia. Histology is the most common technique for identifying these conditions, but it is essential to distinguish between invasive and non-invasive fungal sinusitis. Nasal biopsies are routinely taken from inflammatory masses to confirm or rule out granulomatous diseases. Pathologists must be aware of the diagnostic histological and clinical features of granulomatous sinonasal disease, as it has a broad differential diagnosis. This review examines the pathophysiology and histopathology of inflammatory non-infectious disorders of the sinus tract, including nasal perforations, granulomatous vasculitides Wegener, chronic rhino sinusitis, eosinophilic angiocentric fibrosis, and recurrent polychondritis. To better understand the data, pathologists can focus on molecular pathways and connections related to clinical, genetic, and environmental factors influencing patients' illnesses. A deep learning system has been developed to diagnose maxillary sinusitis, ethmoid sinusitis, frontal sinusitis from the Caldwell and Waters viewpoints. The system can simultaneously recognize and classify each paranasal sinus, eliminating the need for human cropping. The pathogenesis and histology of inflammatory sinus diseases are examined in this review. From the perspectives of Caldwell and Waters, a deep learning system was created to diagnose maxillary sinusitis, ethmoid sinusitis, and frontal sinusitis. The system was trained and validated using a sinusitis percentage of 34.2, then tested on datasets having a sinusitis percentage of 29.4%. The technology does not require human cropping because it is able to identify and categorize each paranasal sinus. Using the Caldwell and Waters, the computer can simultaneously recognize and classify each paranasal sinus.

Keywords: Machine Learning, Deep Learning, Artificial Intelligence, Paranasal Sinusitis, Diagnosis, Fungal Diseases.

1. Introduction

Many frequent disorders that present to head and neck doctors can be among the large variety of diseases that present with sinusitis and/or rhinitis. In addition to knowing how typical diseases present, a pathologist must also be able to identify uncommon or rare diseases that call for specialized care. The normal anatomy and histology of the sinuses and nasal cavities are reviewed in this overview before the many infectious and non-infectious causes of

sinus inflammation are discussed. (Table 1)

2. Components and Method

A collection of 4,870 patients had PNS X-rays utilising Waters' View, including 2,530 subjects with maxillary sinusitis and 2,870 subjects without it. Subsets of the datasets were selected at random to form learning (69%), verification (16%), and testing (14%). Using three different multiple convolutional neural network (CNN) models—VGG-16, VGG-19,

and ResNet-101—we built the majority decision technique to arrive at a fair consensus. Activation maps and quantitative accuracy (ACC) were used to evaluate the sinusitis detection capacity [1-3].

Table 1 Infectious and Non-Infectious Causes of Sinus Inflammation

<p>Rhinosinusitis Caused by Infection</p> <ul style="list-style-type: none"> • Ichthyosporia • Viruses • Bacteria • Fungi • Protozoa
<p>Rhinosinusitis Without Infection</p> <ul style="list-style-type: none"> • Eosinophilia syndrome (NARES) and allergic rhinitis • Non-allergic rhinitis • Hormone, emotional, and food-related rhinitis • Non-allergic, non-eosinophilic rhinitis • Gastro-oesophageal reflux disease • Sensitive (or non-sensitive) work environments • Drug-induced eosinophilic angiocentric fibrosis • Aspirin-induced rhinitis medicamentosa • Cocaine-induced midline destructive lesion
<p>Systemic Illnesses Linked to Rhinosinusitis</p> <ul style="list-style-type: none"> • Primary ciliary dyskinesia • Cystic fibrosis • Diseases causing muco-ciliary dysfunction • Wegener's granulomatosis • Sarcoidosis • Churg-Strauss syndrome • Relapsing polychondritis

2.1. The Histology and Anatomy of Surgery

Particulate matter is removed and the air is made more humid by the nasal cavities. The palatine, maxillary, and ethmoid bones, which support the three turbinates, form the lateral walls of the cavities, while the hard palate forms the floors. The cavities are encircled by bone and cartilage. The meati situated beneath the turbinates serve as the draining

sites for the nasolachrymal duct (inferior meatus), additional ethmoidal cells, maxillary and frontal sinuses (middle meatus), and posterior ethmoidal sinus (superior meatus). Behind the superior turbinate, the sphenoidal recess receives the drainage from the sphenoid sinus. A significant amount of sinus pathology is caused by obstruction to drainage caused by anatomical variance or mucosal illness around the narrow ostial meati. With flexible nasendoscopy and functional endoscopic sinus surgery (FESS), doctors may see sinus illness and has enhanced the caliber of surgery to enhance nasal drainage and eliminate sick tissues. Nerves, arteries, and seromucinous glands are found in the mucosal lining of the sinonasal tract (Figure 1). Compared to the nasal cavities, the sinus lining is thinner and less vascularized (Figure 2). Constructed from ectoderm, the sinonasal (Schneiderian) epithelium lines the sinuses and nasal cavities in children, while the olfactory epithelium lines the nasal cavity. Both types of epithelium are pseudostratified and ciliated columnar. Squamous metaplasia of the nasal vestibule is caused by exposure to airborne particles during the first twenty years of life. About 200 cilia, which protrude into the mucus gel phase and beat in unison at a frequency of 10–20 Hz, are present on the luminal surface of a typical columnar cell [4-6].

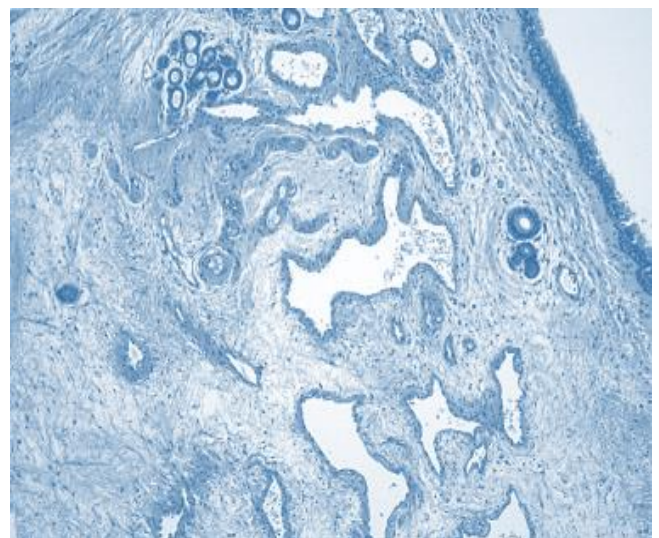


Figure 1 The Nasal Mucosa in a Normal State Has Many Vessels and is Covered in Respiratory Epithelium

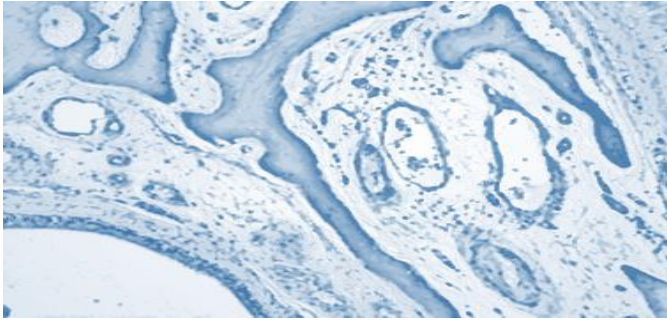


Figure 2 Thinner and Tightly Aligned with The Bone is the Typical Sinus Mucosa

2.2. Sinusitis and Infectious Rhinitis

Fluid leakage from the nasal mucosal glands and arteries is linked to acute viral infection, most usually caused by adenoviruses, echoviruses, or coronaviruses. Infection by certain fungus, bacteria, and other organisms is rare in the industrialized world, although it can occur in biopsies from patients who have moved from or traveled through nations where these illnesses are endemic.

2.3. The Tuberculous Disease

Upper respiratory tract tuberculosis is uncommon, typically connected to lung illness, and can cause polyps, ulcers, or septal perforation. One Under a microscope, there are granulomas of epithelioid and large cells, but there is little evidence of caseous necrosis. Since organisms are rarely observed, the diagnosis is made using molecular testing, culture, and/or clinic-pathological correlation. Other granulomatous disorders are included in the differential diagnosis. (Table 2)

Table 2 Examples of Mycobacterial Infections

Leprosy and tuberculosis are examples of mycobacterial infections
Cyanoscleroma
HIV (human immunodeficiency virus)
Aspergillus flavus fungal infection
The sarcoidosis condition
Wegener's granulomatosis
Churg-Strauss angina
Midline damaging lesion brought on by cocaine
Misuse of drugs through the nose
Paranasal sinuses cholesterol granuloma (post-haemorrhage)
Appropriateness

2.4. Leprosy

Aerosols produced by upper respiratory tract diseases carry the Mycobacterium leprae bacteria. Many infections enter the nose through the nasal mucosa, and nasal diseases might manifest years before skin diseases. The majority of nasal lesions are seen in anergy-affected people with lepromatous leprosy, which is characterized by fibrosis, neutrophils, eosinophils, plasma cells, and mucosal macrophages packed with acid-fast bacilli. Tuberculoid leprosy is present in patients with a strong T-cell mediated immune response. The clinical characteristics, organism-specific stains, and/or molecular testing are used to make the diagnosis.

2.5. Syphilis of the Nose

In certain regions of Eastern Europe, North and Central Africa, and sections of Central and South America, rhinoscleroma is endemic. The gram-negative bacteria Klebsiella rhinoscleromatis is the cause of the disease, which typically affects the lip, oropharynx, nasopharynx, and nasal cavities. There are three stages to the illness. Ulceration, necrosis, acute inflammation, and granulation tissue are all present in the rhinitic phase. The florid or granulomatous phase is characterized by a strong mixed inflammatory infiltration of lymphocytes, plasma cells, and macrophages as well as pseudoepitheliomatous hyperplasia. The big, vacuolated macrophages (Mickulicz cells) (Figure 1) contain numerous bacilli that are visible on Warthin–Starry, gram, or Giemsa stains and verified by culture. Russell bodies are also conspicuous in the plasma cells. There are few Mickulicz cells and varied fibrosis in the last, fibrotic phase (Figure 3).

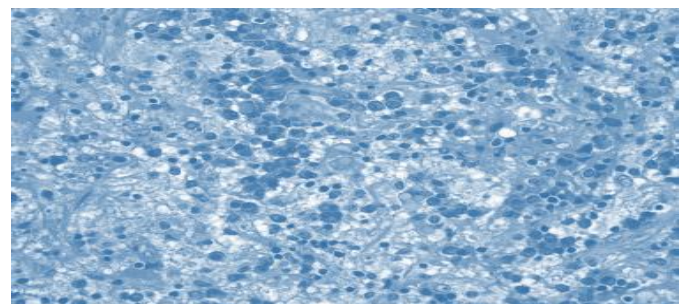


Figure 3 Rhinoscleroma Displaying Big Lymphocytes, Plasma Cells, and Vacuolated Macrophages

2.6. Rhinitis

Despite Seeber's initial description in 1900, identifying the causative organism *Rhinosporidium seeberi* has proven difficult. Molecular taxonomy using 18S rRNA sequencing has placed this organism within the group of protists known as Ichthyosporaea, which typically infect fish and amphibians. In India and Sri Lanka, rhinosporidiosis is endemic and commonly manifests as sinus and ocular infections. Nasal infections present with thick mucosal tissue covered by overgrown squamous or respiratory epithelium, accompanied by significant infiltration of lymphocytes and plasma cells. The disease is characterized by numerous cysts (sporangia) ranging from 100 to 300 μm in diameter, possessing thick walls that stain positive for PAS, and containing abundant endospores (Figure 4).

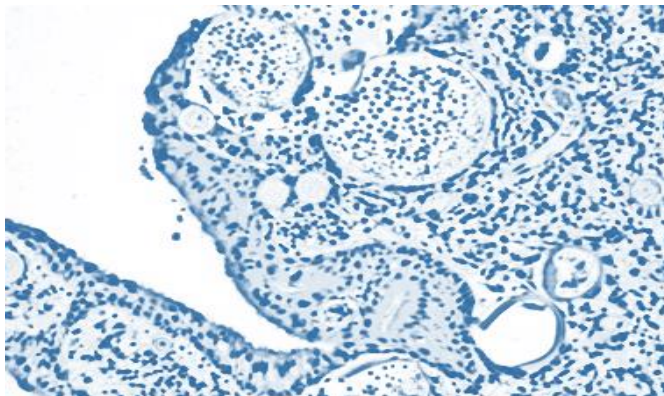


Figure 4 Indicative of Rhinosporidiosis are Large Sporangia Containing Endospores within The Superficial Mucosal Tissue

2.7. Fungus Illnesses

Although the complexity of the interactions between various fungal species and the human immune system are not fully understood, the classification of fungal-related disorders of the nose and paranasal sinuses is significant for prognosis and treatment. Consequently, the diagnosis of fungal sinusitis depends on the histological identification of fungus in sinus tissue. Fungus are common airborne allergens and can be cultured from the nasal secretions of most healthy individuals⁷. Special stains (Grocott and diastase-PAS) should be used regularly when analyzing sinonasal biopsies, especially those from

immunocompromised persons, as the density of fungal elements varies from sparse to extensive. It is rarely possible to discriminate between different fungal species by the shape of the hyphae; instead, fungal cultures must always be used. The asymmetrical wide hyphae illnesses linked to *Aspergillus* sp. and the dematiaceous fungus are characterized by typical dichotomously branching septate hyphae of *Mucor* sp.

3. Results and Discussion

3.1. Results

3.1.1. Patient Collections

sums up the fundamental characteristics of the patient. There were 665 women (48.2%) and 732 men (50.2%) in the initial and final evaluation sets, and 76 women (57.2%) and 58 men (41.5%) in the test set. For the training and validation sets, the average age was 51 ± 18 years, whereas for the test set, it was 55 ± 16 years. Features of the patient and the training, validation, and temporal test set label distribution.

3.1.2. Deep Learning Model Performance Comparison

Enumerates the deep learning algorithm's performance. The single primary view for frontal, ethmoid, and maxillary sinusitis as well as the single secondary view for frontal sinusitis were comparable with the AUCs of the MV-based deep learning method, which was higher than those of the single secondary view for maxillary and ethmoid sinusitis.

3.1.3. With ACC and Activation Maps

With ACC and activation maps, we contrasted the outcomes of our methods. The analyses of the internal test dataset revealed that the ACC [and area under the curve (AUC)] for VGG-16, VGG-19, ResNet-101, and the majority decision were, respectively, 86.3% (0.882), 91.7% (0.889), 92.6% (0.936), and 95.0% (0.947). 86.57% (0.875), 86.57% (0.876), 91.11% (0.930), and 93.12% (0.940) were the ACC (and AUC) of the external test dataset for the majority decision, VGG-16, VGG-19, and ResNet-101, respectively. By applying the majority decision's compensation function, algorithms for making majority decisions are able to identify absent lesions and fix them. According to the assessments of the two radiologists, there was excellent agreement about the reproducibility of the sinusitis labeling. The



majority decision with several CNN models is displayed, along with the performance evaluation of the training and validation datasets for the VGG-16, VGG-19, and ResNet-101 CNN models. 98.9% and 86.7% for the VGG-16 model, 98.7% and 91.6% for the VGG-19 model, and 98.8% and 89.9% for the ResNet-101 model were the estimated ACCs of the training and validation datasets. For both the training and validation datasets, the performance of the majority decision was assessed at 98.9% and 91.2%, respectively.

Table 2 Dataset/Model

Dataset/Model	VGG-16%	VGG-19%	ResNet-101%	Manjority Decision%
Instructional Set	98.9	98.7	98.8	98.9
Collection of verification	86.7	91.6	89.9	91.2

The majority decision process and each CNN model's performance are assessed using training and validation datasets.

3.2. Discussion

In the test datasets, the activation map analysis revealed that the VGG-16 and VGG-19 models identified a comparatively bigger region than the actual lesion. In contrast, a lesion that the VGG-16 or VGG-19 models missed may also be recognized by the ResNet-101 model, which similarly detected a comparatively smaller region than the real lesion. It was demonstrated that by balancing the benefits and drawbacks of every deep learning model, the majority decision method was efficient in arriving at a suitable conclusion. After comparing the classification accuracy for normal participants with an activation map, a normal characteristic identified the surrounding areas instead of the maxillary sinus region. It is demonstrated why CNN models identify the distinctions between sinusitis and normal as a primary property of the maxillary sinus's comparatively bright signal intensity. Our study aims to ensure dependability by displaying the normal situations using several algorithms, whereas previous articles simply displayed abnormal cases with a heat map. To ensure repeatability, the external test dataset

from several medical centers was excluded in the first place. Depending on the maker or model, there could be a slight variation in X-ray equipment's performance when compared to other medical imaging equipment. The external test dataset from other medical centers was consequently excluded from this investigation. For example, if a nearby medical facility is still operating with outdated technology, then employing artificial intelligence (AI) assistive software will also need an additional performance test. Furthermore, only maxillary sinusitis was evaluated by the optimal majority decision technique that was proposed. Evaluating sinusitis in the frontal, ethmoid, and sphenoid regions is therefore limited. This study has various restrictions. First, for reproducibility, the external test dataset from several hospitals was excluded. Depending on the manufacturer or model, there may be a slight variation in the performance of X-ray equipment when compared to other medical imaging equipment. Therefore, the external test dataset from other medical centers was excluded from this investigation. However, in the instance of a nearby medical facility employing rather antiquated technology, an extra performance assessment is also necessary in order to make use of artificial intelligence (AI) assistive software. Secondly, the algorithm for majority decision that was suggested was fine-tuned to assess solely maxillary sinusitis. As such, the evaluation of sinusitis in the frontal, ethmoid, and sphenoid regions is limited. More research is being done because sinusitis at various regions needs to be evaluated in addition to the maxillary in order to apply AI-based assistive software in the future. Thirdly, deep learning black-box solutions such as pattern recognition and representation techniques are absent. In order to solve the black-box dilemma, it must come to an acceptable consensus. The deep learning black-box problem was resolved through the use of feature recognition-based activation maps. As the results demonstrate, this leads to the expression of both lesion location and classification. It facilitates the appropriate deduction of the deep learning analysis by medical specialists. To comprehend every step of the deep learning process is insufficient, though. For example, it is



challenging to comprehend each taught CNN model's pattern. We can optimize the AI system as a whole and comprehend the benefits and drawbacks of each model by knowing how well it recognizes patterns. In order to get over this restriction, each layer needs have access to a feature connectivity representation that shows which feature weights are strong. Convolutional recurrent neural network (CRNN), a hybrid of CNN and recurrent neural network (RNN), can be used in conjunction with feature representation to help text-based description algorithms get over the black-box constraint in medical applications. When compared to individual CNN models, a majority decision method utilizing multiple CNN models demonstrated much higher accuracy in lesion diagnosis. As an additional tool, the suggested deep learning technique utilizing PNS X-ray pictures can help increase the precision of the maxillary sinusitis diagnosis.

Conclusion

On Waters' and Caldwell view radiographs, our deep learning algorithm was able to accurately diagnose frontal, ethmoid, and maxillary sinusitis; in fact, the algorithm performed better than radiologists in the cases of ethmoid and maxillary sinusitis. On reasonable request, the corresponding author will make the datasets created and/or analyzed during the current study available, however access to them is contingent upon approval from the collaborating institutions' institutional review boards. Radiology free-text reports can be classified by a deep learning CNN model with comparable accuracy.

Acknowledgements

The authors are grateful to Read Brain Co., Ltd. for providing deep learning analysis advice. Every author says they have no conflicting interests with the business. Funding: The Basic Science Research Program through the Ministry of Education of the Republic of Korea (NRF-2016R1D1A1B03933173 and 2018R1D1A1B07041308) and a grant from Kyung Hee University in 2015 (KHU-20150828) provided funding for this work.

References

[1]. Fagnan LJ. Acute sinusitis: a cost-effective approach to diagnosis and treatment. *Am Fam Physician* 1998; 58:1795-802, 805-6.

- [2]. Kirsch CFE, Bykowski J, Aulino JM, Berger KL, Choudhri AF, Conley DB, Luttrull MD, Nunez D, Jr, Shah LM, Sharma A, Shetty VS, Subramaniam RM, Symko SC, Cornelius RS. ACR Appropriateness Criteria((R)) Sinonasal Disease. *J Am Coll Radiol* 2017;14:S550-S559. 10.1016/j.jacr.2017.08.041
- [3]. Anand, V.K. Epidemiology and economic impact of rhinosinusitis. *Ann. Otol. Rhinol. Laryngol. Suppl.* 2004, 193, 3–5.
- [4]. Merrell, R.A.; Yanagisawa, E. Radiographic anatomy of the paranasal sinuses. I. Waters' view. *Arch. Otolaryngol.* 1968, 87, 184–195.
- [5]. Yanagisawa, E.; Smith, H.M. Radiographic anatomy of the paranasal sinuses. IV. Caldwell view. *Arch. Otolaryngol.* 1968, 87, 311–322.
- [6]. Burke, T.F.; Guertler, A.T.; Timmons, J.H. Comparison of sinus x-rays with computed tomography scans in acute sinusitis. *Acad. Emerg. Med.* 1994, 1, 235–239.